Experimental analysis of operational data for roundabouts through advanced image processing

# Journal Pre-proof

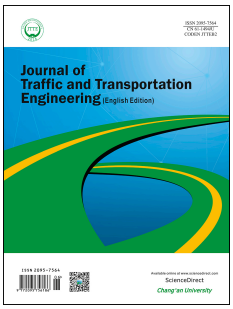


Experimental analysis of operational data for roundabouts through advanced image processing

Marco Bassani, Lorenzo Mussone

PII: S2095-7564(18)30426-4

DOI: https://doi.org/10.1016/j.jtte.2019.01.005

Reference: JTTE 266

To appear in: *Journal of Traffic and Transportation Engineering (English Edition)*

Received Date: 9 September 2018

Revised Date: 22 January 2019

Accepted Date: 28 January 2019

Please cite this article as: Bassani, M., Mussone, L., Experimental analysis of operational data for roundabouts through advanced image processing, *Journal of Traffic and Transportation Engineering (English Edition)*, https://doi.org/10.1016/j.jtte.2019.01.005.

Original research paper

# Experimental analysis of operational data for roundabouts through advanced image processing

Marco Bassani[a], Lorenzo Mussone[b,*]

[a] *Department of Environment, Land and Infrastructure Engineering, Politecnico di Torino, Torino 10129, Italy*

[b] *Department of Architecture, Built Environment and Construction Engineering, Politecnico di Milano, Milano 20133, Italy,*

**Highlights**

- An investigation carried out to survey vehicle movements at roundabouts was presented.
- O/D matrix, classification, trajectories tracking, speed and acceleration from video images analysis.
- A number of camera set-up configurations were adopted.
- Performance of installation set-ups with different vehicle tracking strategies has been evaluated.

**Abstract**

Roundabout is still the focus of several investigations due to the relevant number of variables affecting their operational performances (i.e., capacity, safety, emissions). To develop reliable models, investigations should be supported by devices and related sensors to extract variables of interest (i.e., flow, speed, gap, lag, follow-up time, vehicle classification and trajectory). Notwithstanding that several sensors and technologies are currently used for data collection, most of them present limitations. The paper presents the investigation carried out to survey vehicle movements at roundabouts as a comprehensive video image analysis system is able to derive the origin/destination

(O/D) matrix, compile a vehicle classification, track individual vehicle trajectories together with corresponding speeds and accelerations along paths. To this end, the authors collected video-sequences that were analyzed with a piece of software developed for that task. To minimize the problems due to perspective distortion, environmental effects, and obstructions, a number of camera set-up configurations were adopted with equipment being placed on central or external poles, and on permanent fixtures such as raised working platforms outside the confines of the intersection area. Performance of those installation set-ups with different vehicle tracking strategies has been evaluated. Particularly, speed has been successfully related to trajectory tortuosity, the result of which emphasizes the tremendous potential of image analysis and opens up to further studies on the evaluation of the operational effects of roundabout geometrics.

**Keywords:**

Transportation; Roundabout; Image analysis/processing; Vehicle tracking and classification; Operating speed; Trajectory.

* Corresponding author. Tel.: +39 02 2399 5182; fax: +39 022 399 5195.

E-mail addresses: marco.bassani@polito.it (M. Bassani), lorenzo.mussone@polimi.it (L. Mussone).

## 1 Introduction

In many countries, roundabouts have increasingly become the intersection of choice due to the positive and acknowledged operational benefits deriving from their geometrics as reported in literature (Curti et al., 2008; Rodegerdts et al., 2010, 2014). Nevertheless, operational performance in terms of capacity, speed, and safety still remains a focus of investigation due to the number of variables, apart from geometric ones, affecting trajectories and speeds of crossing vehicles (Sacchi et al., 2011), and emissions (Fernandes et al., 2015; Salamati et al., 2013).

With the objective of developing reliable models, investigations should be conducted using robust tools and with attention being paid contextually to the circulating roadway and all the legs. Such tools have to be able to: (a) extract traffic variables of interest such as flow, speed, gap, lag, follow-up time, vehicle length and weight, as well as vehicle position in time (i.e., vehicular trajectory); (b) ensure that the recording video system is not visible to drivers so as to avoid any behavioural effects; and (c) contribute to a reduction in the resources needed to run the system, also in terms of operator time.

Although several sensors and technologies are currently used for traffic data collection in roundabout, most of them are limited in their ability to survey traffic variables, a point which is discussed in the paper. In order to avoid the limitations associated with their use, video recording surveys and related image processing techniques can be successfully employed (Messelodi et al., 2005; Migliore et al., 2006; Mussone et al., 2013).

The paper proposes a methodological contribution to analyse speed and trajectories of vehicles through roundabouts. It presents the activities undertaken by the authors in the development and use of a video recording system in conjunction with a software developed for the derivation of: (a) the origin/destination (O/D) flow matrix, (b) the vehicle classification, and (c) the trajectories and associated speeds and curvature diagrams along the paths traversing a roundabout.

## 2 Background

### *2.1 Vehicle position data collection tools*

At present, many multi-purpose detectors for traffic data collection are available at affordable prices. Laser, radar, microwaves, infrared, acoustic, ultrasonic, capacitive, piezoelectric, magnetometric, and magnetic loops are the technologies employed in sensors. With more or less similar levels of efficiency and precision, all the above-mentioned technologies allow for the collection of macroscopic variables such as flow, speed, density (or occupancy) and vehicle specific variables such as headway, gap, lag, follow-up time and vehicle length and weight.

Their main disadvantage (apart from the fact that they sometimes need to be physically supported or that, in some cases, their installation can occasionally lead to an intrusion into the traffic circulation area) is that their measurements refer to a single road section or linear segment, and therefore multiple measurement points require an array of collection tools. None of them, in fact, may be employed for vehicle tracking, especially in situations where vehicles move along inflected trajectories (e.g., in case of roundabouts). This would not be a serious problem unless it is strictly necessary that information gathered by detectors relates uniquely to each individual vehicle. This task is particularly crucial at roundabouts where the construction of the O/D matrix is very challenging (Grenard and Wei, 2012).

One possible way to track vehicles could be the floating car data method that, however, requires that a statistically significant number of vehicles are equipped with positioning sensors i.e., global positioning system-global navigation satellite system (GPS-GNSS), inertial measuring unit (IMU) or combined sensors, with data recorded on board and/or transferred to a central system. With this method, installations and experiments are expensive and complicated since it (the method) needs a large number of vehicles together with the participation of the general public to be of any use in a realistic setting. However, the current wide diffusion of navigation systems working in real time and connected to a central unit makes this feature of increasing interest for the near future, at least for transport planning purposes (average speed prediction and O/D matrix reconstruction). Other emerging survey technologies, such as the 3D light detection and ranging (LiDAR), facilitate the

collection of clouds of data and could be used to track vehicles. At present, however, they are more expensive than video-image technology and entail a higher level of complexity and effort in the collection and modelling of a large quantity of data.

Consequently, the most promising methodology available at present for the tracking of vehicles is certainly represented by the video analysis technique. Several contributions have demonstrated that it may be employed in a variety of applications from simple vehicle detection (Messelodi et al., 2005; Wei et al., 2005) to the gathering of comprehensive data for trajectories in both time and space domains, thus allowing a complete reconstruction of movements along sections (Beymer et al., 1997) and at vehicle intersections (Alhajyaseen et al., 2013; Apeltauer et al., 2015; Datondji et al., 2016; Dinh and Tang, 2017; St-Aubin et al., 2013) or cyclist behaviour trajectory analysis (Sakshaug et al., 2010; Zaki et al., 2013).

With the aim of providing information useful for the calibration of microscopic simulation models, Alhajyaseen et al. (2013) analysed the relationship between speed and trajectory at at-grade urban intersections. Adopting the survey technique described in Suzuki and Nakamura (2006), those authors demonstrated the effect on vehicle trajectory of geometry (angles between legs, corner radii, number of exit lanes, and positions of hard noses of the medians) for different vehicle types negotiating the intersection at different speeds, confirming the potential of the image analysis technique when conducting surveys to gather positioning data at road junctions. In Mussone (2013), the question of visibility on roundabouts was faced by using real trajectories extracted from video image records.

Finally, the possibility to track vehicles in roundabouts by video cameras mounted on drones has raised a certain interest. Guido et al. (2016) used them to detect and compare tracking data with GPS-equipped vehicles only. According to the authors, the methodology is promising but needs to be improved for removing noise and inaccuracies due to uncontrolled movements and vibrations of drones under the effects of wind.

### *2.2 Position and speed data modelling at roundabouts*

Operational data for modern roundabouts were investigated for the first time in the National Cooperative Highway Research Program (NCHRP) Project 3-65, when a comprehensive inventory of

129 103 US roundabouts with geometric, operational, and safety data was carried out (Rodegerdts et al.,
130 2007). Of these, 31 roundabouts were the focus of video recordings in the spring and summer of 2003,
131 with 34 h of traffic operation data accumulated (i.e., flow measurements, gaps, delays and travel times,
132 turning movement proportions, and vehicle types). For this purpose, a video recording system
133 consisting of analogic and digital video cameras was used. Operational data were recorded making
134 use of "event recording" software (Rodegerdts et al., 2006). In the same study, sixteen single-lane and
135 eleven multi-lane roundabouts were considered for the operating speed surveys (Fig. 1).

136 In Rodegerdts et al. (2007), speed data were collected through the use of radar guns only at four
137 specific locations: one outside (i.e., at 60 m from the yield line) and three inside the roundabouts. In
138 particular, as seen in Fig. 1, they were collected at the yield line (section 1), at the midpoint of the
139 adjacent splitter island (section 2), and at the exit (section 3), with a minimum number of speed data
140 per section greater than 30 to achieve a statistical significance. Speed data collected at the
141 roundabouts were differentiated both by movement type (i.e., left, through or right turn), and by vehicle
142 type (i.e., passenger cars, trucks), and only passenger car data were used for that analysis.

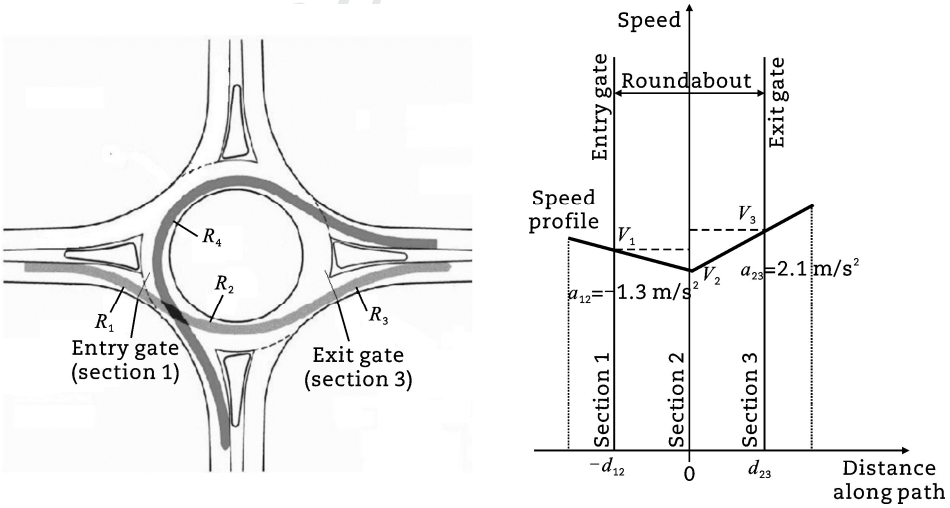


143

144 **Fig. 1** Layout of the operating speed surveys (Rodegerdts et al., 2010). (a) Geometric characteristics of trajectories. (b) Schematic speed
145 profile.
146

147 Starting from the elementary arc with the minimum radius on which the minimum speed is reached
148 in the circulatory roadway ($V_2$), speeds at the entry ($V_1$) and exit ($V_3$) gates can be derived under the

hypothesis of naturally decelerated/accelerated motion and adopting average deceleration ($a_{12}$) and acceleration ($a_{23}$) values from observational data (Robinson et al., 2000).

The predictive speed equations (Rodegerdts et al., 2007) for the through movement for entry ($V_1$) and exit ($V_3$) speeds in km/h (Fig. 1) are

$$V_1 = \min\left\{V_{1\text{base}};\ 3.6\sqrt{\left(\frac{V_2}{3.6}\right)^2 - 2a_{12}d_{12}}\right\} \quad (1)$$

$$V_3 = \min\left\{V_{3\text{base}};\ 3.6\sqrt{\left(\frac{V_2}{3.6}\right)^2 + 2a_{23}d_{23}}\right\} \quad (2)$$

where $a_{12}$ is the deceleration between the point of interest of the entry path and the midpoint of the path (assumed equal to −1.3 m/s$^2$), $a_{23}$ is the acceleration between the midpoint of the path and the point of interest of the exit path (assumed equal to 2.1 m/s$^2$), and $d_{12}$ and $d_{23}$ are the distances between the points of interest along the entry and exit paths, and the midpoints of these paths respectively, which are measured along the vehicle trajectory. In Eqs. (1) and (2), $V_{1\text{base}}$, $V_2$ and $V_{3\text{base}}$ represent the predicted speeds at the entry, midpoint and exit points based on path radii $R_1$, $R_2$ and $R_3$ (Fig. 1) using the basic formula of vehicle equilibrium on curves (Eq. (3)).

$$\begin{cases} V_{1\text{base}} = \sqrt{gR_1(f+q)} \\ V_2 = \sqrt{gR_2(f+q)} \\ V_{3\text{base}} = \sqrt{gR_3(f+q)} \end{cases} \quad (3)$$

where $g$ is the acceleration of gravity (equal to 9.81 m/s$^2$), $f$ is the side friction factor, and $q$ is the super-elevation, which is normally −2% in the case of modern roundabouts (Rodegerdts et al., 2007). Eq. (3) may also be used to evaluate the speed along a left turn movement, using the value of $R_4$ indicated in Fig. 1 as a radius.

A comparison between the 85th percentile speed observed in the field and the corresponding values predicted using Eqs. (1) and (2) demonstrated that the proposed model was applicable to those maneuvers in which vehicles interact with the central island (left turn and through movements), and that it was considered conservative because it tends to overestimate the operating speed. The regression analyses performed on these models with available data showed the coefficients of determination to be too low, thus indicating that the variables considered could not provide a reliable

prediction of speed on the circulatory roadway. This leads to the conclusion that the evaluation of operating speed at roundabouts still remains a challenge at both the analysis level and design stage (Šurdonja et al., 2018; Perco et al., 2012).

Currently, TORUS (Transoftsolutions, 2018) and CIVIL 3D (Autodesk, 2018) software packages consider the fastest path analysis according to literature (Robinson et al., 2000; Rodegerdts et al., 2007). These programs calculate the expected speed on the circulatory roadway along the minimum radius along the "fastest vehicle path", which represents the smoothest possible trajectory of a vehicle, in the absence of other vehicles and ignoring all lane markings, from the entry to the exit gates (Ahac et al., 2016; Rodegerdts et al., 2006).

## 3 Methodology

Starting from this literature review, the authors proposed a comprehensive methodology to collect video records from existing roundabouts and derive information useful to model the relationship between speeds and trajectories of vehicles. The tracking of trajectories gives also the possibility for the derivation of trajectory tortuosity parameters, as well as the reconstruction of O/D matrix. From the length of moving objects in the road scene, a neural network was trained to classify vehicles along each movement.

To minimize the problems due to perspective distortion, environmental effects, and obstructions, a number of camera configurations were adopted with equipment being placed on central or external poles (with respect to central island), or on permanent fixtures such as raised working platforms outside the confines of the intersection area. Strengths and weaknesses of the selected installations are described in order to determine the optimal set-up. Three case studies in Northern Italy were considered. Up to three video cameras were used in different set-ups. Each installation exhibited a different behaviour under the effects of wind, cloud cover, shadows, dazzle, perspective deformation, and obstructions. Two additional aspects, namely ease of perspective correction and synchronization between video cameras, were also investigated and solved.

An important issue faced in the paper is the synchronization of recorded images when using more than one video camera. This was achieved by inserting a timestamp for every recorded stream. This

200 task is easier when cameras are mounted on the same pole and camera output can be connected
201 directly to the same computer. More demanding is the case when several cameras on different poles
202 are involved and a wireless connection is needed to link the computers together to use the same
203 timestamp. Besides this, the authors experimented two different strategies in order to build trajectories:
204 by merging trajectories extracted by separated images (MT) and blending images before extracting
205 trajectories (BI).

206 Finally, the data collected from image analysis in the three case studies have provided general
207 relationships between speeds and trajectories as affected by roundabout geometrics. Differently from
208 the approach of Robinson et al. (2000) and Rodegerdts et al. (2007), continuous speed and trajectory
209 data help the authors in the development of a new model able to relate speeds to trajectory tortuosity.
210 The possibility to work out such a model can be considered by analysts and designers as an
211 opportunity to predict speed behaviour of drivers along their path on the basis of roundabout
212 geometrics.

213 *3.1 Survey tools and methodology*

214 The instrumentation used to collect and evaluate data consists of a vision system and a real time
215 kinematics-global positioning system (RTK-GPS), both connected to a dedicated PC (Fig. 2). In
216 Mussone et al. (2011, 2013), a more detailed description of the system, including details of both
217 hardware and software characteristics, can be found. Images from video cameras must not have blind
218 spots and this condition can be achieved through a planned set up of optics and video camera
219 orientation.

220 The vision system (Fig. 2(a)) consists of one to three cameras with a resolution of 1360 x 1024
221 pixels. The optical lens of each video camera was adjusted in line with the application scenario by
222 remote control. The vision system provided information on vehicular flow through the processing of
223 images recorded by the video camera(s), while the RTK-GPS system was used to generate data
224 useful for calibrating and evaluating the vision system.

225 The RTK-GPS system (Fig. 2(b)) is composed of a base station equipped with a Trimble MS750
226 GPS and a Trimble Zephyr Antenna. A rover, made up of a Trimble 5700 GPS (working at 5 Hz) and a

Trimble Zephyr Antenna, is attached to a probe vehicle and connected via radio link (DiGi XBee Pro modules in point to point mode) to the base station.

(a) (b)

**Fig. 2** Data collection and evaluation instrumentation. (a) Vision system placed upon a raised working platform. (b) The probe vehicle with the rover system.

In order to improve the process of matching video camera data with GPS data, a series of marked points visible in video images were drawn on the pavement surface of the roundabout (four points on each leg, and from four to eight points on the circulatory roadway depending on the dimension(s) of the central island). The exact positions of these points were, then, attained by both GPS (with an accuracy ranging from 2 to 15 cm) and by video recording. The matching of vehicle coordinates (and then speed) data calculated by image processing with the data gathered by GPS was then a relatively straightforward task.

Calibration of the vision system was carried out for image rectification, thus tuning the Bouguet camera model of the vision system. Image rectification aims at achieving homogeneity in terms of corresponding pixels in the image plane, and the ratio between lines lengths and angles in a specific plane of the observed world (i.e., the central islands is circular but it appears an ellipse in the perspective projection). This requires a proper image transformation, i.e., a homography between the road surface and the image plane. Vehicle tracking on the transformed plane turns out to be quite

effective and more accurate than when carried out on the original image. The homography is known when the size and the position of some specific elements of the observed scene are available.

### *3.2 Pre processing*

The images gathered require conversion, undistortion, and rectification, while RTK-GPS data need data conversion (for rover data) and synchronization between base station and rover timestamps.

The image analysis was carried out by a software (developed at Politecnico di Milano and based on MATLAB platform) named Vehicle Tracking for Roundabout Analysis (VeTRA), which employs genetic algorithm optimization procedures to minimize the re-projection error of the central island onto the image plane, and also provides a complete projective transformation from the 3D real world to the 2D image, by constraining world points to lie at ground level.

The current version of VeTRA has further improved performance in blob recognition with respect to the original version used in Mussone et al. (2011). Improvements to the algorithms have now limited the negative effects of some environmental factors (i.e., wind, sudden changes in light conditions due to clouds), occlusions due to fixed objects (i.e., trees, poles) and moving vehicles (Oh et al., 2012), as well as perspective deformations.

The key tool in VeTRA is its tracking system, which detects moving objects in the field through an adaptive background modelling and subtraction algorithm. The image areas representing the vehicles (known as “blobs” in information science jargon) are identified in the foreground through shadow and noise removal. The tracking system is capable of distinguishing between newly detected blobs and previously tracked vehicles between three types of vehicles as explained in the next paragraph. The blobs are continuously updated as new information is received. All these activities rely on a proper model of the background, which has to be sufficiently robust to contend with daily changes in light conditions and camera oscillations. Although the tracking system detects the movements of objects in the background, it is able to filter and hence exclude from computation all the small movements of any objects (i.e., trees, sheets on the pavement, etc.) affected by wind.

When more than one video camera is used, two different strategies can be employed to consolidate the information. One strategy merges the blob trajectories extracted from each separate video image

(here called Merging Trajectory (MT) strategy), the second blends images from video cameras before extracting trajectories from the blended images (here called Blend Images (BI) strategy). There are a number of problems and advantages associated with each strategy that were tested in this experiment.

With the MT strategy, the trajectory of the same vehicle is extracted from video cameras (two or more) as in the approach with one camera only. After that, trajectories of the same vehicle are associated and superimposed in order to obtain only one trajectory. The challenging activity is the association of trajectories avoiding strong discontinuities between them.

With the BI strategy, a new image is generated from the blending of all images collected to exclude the portions of images affected by distortion. Then, blended images are analysed as in the one camera approach to extract trajectories.

The MT strategy makes it easier to extract blob trajectories separately from each video camera but does not guarantee a perfect continuum (in the sense of function derivability) of single trajectories. On the other hand, the BI strategy allows a final complete trajectory which is perfectly continuous but requires considerable effort due to merging images. In fact, isomorphic transformation and perspective correction must be applied to each image to maintain the same scale over the trajectory.

It is worth noting that new set-ups with a different number of video cameras required an improvement of the original version of VeTRA (Mussone et al., 2013). The new images produced by blending separate images, or the new trajectories derived from mixing the trajectories given by each video camera, are significant results for the post processing phase.

### *3.3 Post processing I – trajectory reconstruction*

For each video survey, the blob trajectories produced by the tracking system are processed and stored in a database in order to generate the O/D matrix, vehicle trajectories, speed profiles and the vehicle classification.

Trajectories on pavement surfaces are calculated from trajectories between the entry and exit gates of the circulatory roadway on the image plane using RTK-GPS data collected by the rover on the probe vehicle. This was accomplished through a comparison of RTK-GPS and tracking system data, using the synchronization data to obtain the same amount of information. Extracted trajectories are

302 then saved to a system of local coordinates. Speed and curvature profiles are obtained from
303 calculations based on vehicle position and time. Speed is calculated for two consecutive points by
304 simply dividing the distance between them by the elapsed time (equal to the frame rate of the camera,
305 except in those very rare cases where some frames have been lost).

306 The tracking system used in VeTRA follows two different procedures. The first one is less
307 sophisticated and is employed for flow classification purposes as it distinguishes between (a) bikes
308 and motorbikes, (b) light vehicles, vans and campers, and (c) heavy vehicles. It detects the blob for
309 each vehicle, which is then tracked from the entry to the exit section. In this paper, only classes (b)
310 and (c) were used for performance comparison since too few bikes and motorbikes were observed
311 during the survey.

312 Classification is based on vehicle dimension, particularly on its length, which is derived from blob
313 length. Since blob dimension generally changes according to its position inside the image (that is, the
314 position inside the circulatory roadway) due to perspective distortion, a neural network (NN) was used
315 to classify vehicle length by using for training some images sampled from vehicle trajectory,
316 accurately divided by movements. The NN must be trained in every location because it needs to learn
317 the effect of perspective distortion along the circulatory roadway. The accuracy of NN recognition was
318 high with an error lower than 3% for trajectories closer to video camera; higher errors were observed
319 for short trajectories, and for those farther from the video camera where perspective distortions may
320 create difficulties in recognition.

321 The second tracking procedure is more accurate and is employed for trajectory and speed analysis.
322 It recognizes the barycentre (or centroid) of each blob in 2D and produces a continuous curve formed
323 by points that are known in the space and time domains. More details on tracking procedures are
324 available in Mussone et al. (2013).

325 *3.4 Post processing II – data treatment for speed analysis*

326 A filtering algorithm in VeTRA was included to reject trajectories in which the speeds are too low due
327 to vehicle conflict both in the circulatory roadway and in the approaching and departure legs. More
328 specifically, vehicles that stopped before entering or reduced the speed to give priority to circulating

ones were excluded from the speed analysis to obtain free flow speeds only. As a result, trajectories with average speeds between entry and exit lower than 10 km/h were discarded. Filtering was also necessary to exclude stationary vehicles in the circulating roadway, or affected in trajectory by conflicting vehicles. In fact, in some cases, very low speeds were the result of superimposition of trajectories (and blobs) of two or more vehicles.

When available in time and space domains, the trajectory of any isolated vehicle traversing the roundabout in free-flow conditions contains all the information necessary for an assessment of how the said vehicle trajectory was affected by the geometry of the roundabout. Tortuosity indexes may be used to characterize curved trajectories. In this paper, two tortuosity indexes, having as an objective the characterization of the vehicle paths associated with specific maneuvers (crossing, right, left and U-turn), have been derived by reference to general literature. It is obvious that these indexes cannot capture all aspects of driver behaviour but they are helpful in understanding whether the trajectory itself and related vehicular speed are confined to a range within recommended operating intervals.

According to Fig. 3, the first index ($T_1$) (a derivation of index $T_2$, presented hereafter) is shown as follow

$$T_1 = \Sigma_i \left(|\alpha_i|/R_i\right)/L \tag{4}$$

where $|\alpha_i|$ is the absolute value of the angle between the tangents passing from two successive recorded points ($P_i$ and $P_{i+1}$, $P_{i+1}$ and $P_{i+2}$), $R_i$ is the radius of the osculating circle that is derived from thirty points around the considered one (15 before $-P_{i-15}$, ⋯, $P_i$, and 15 after $-P_{i+1}$, ⋯, $P_{i+15}$), $L$ is the length of the trajectory between the entry and the exit gates, and $i$ is one of the considered points. The sum over $i$ includes all the points between the entry and the exit gates. Thirty-one points allow to manage a set of images of one second duration (at the current frame rate), which can be considered long enough to smooth peaks due to random noise effects in blobs.

The second tortuosity index ($T_2$) is obtained with the Eq. (5).

$$T_2 = \Sigma_i(|\alpha_i|/L) \tag{5}$$

Eq. (5) is also known in literature as the curvature change ratio (Yasser and Mohamed, 2011).

(a)

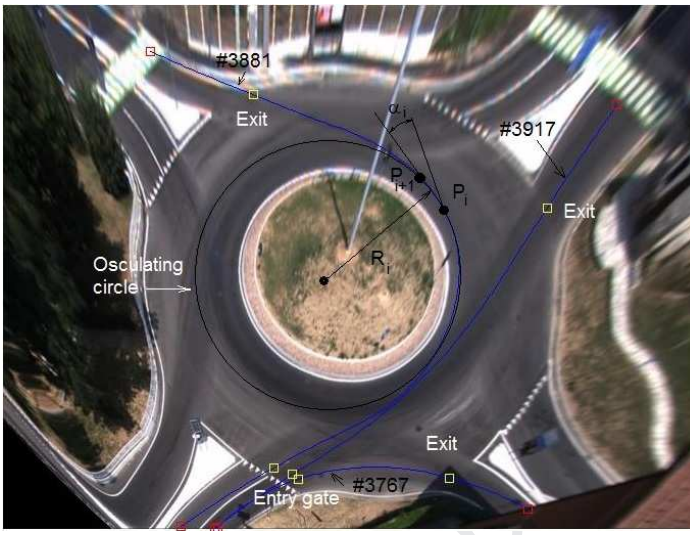


(b)

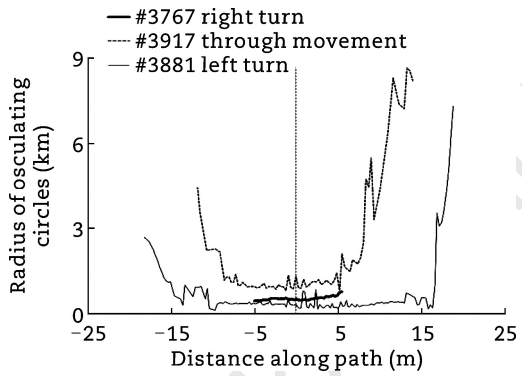


(c)

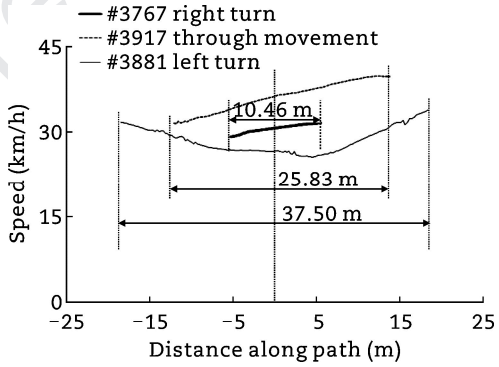


(d)

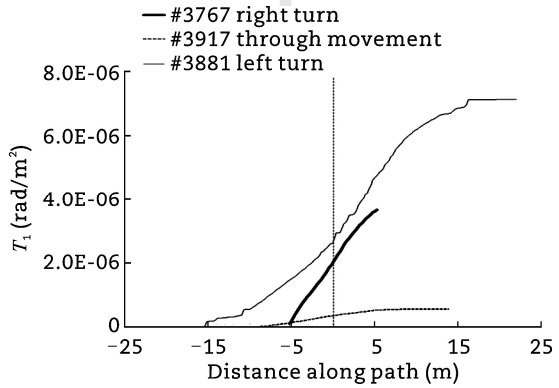


(e)

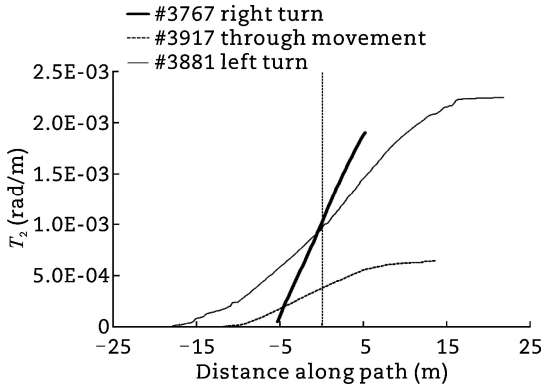


**Fig. 3** Trajectory analysis. (a) Typical curves for parameter analysis. (b) Trajectory radius. (c) Speed. (d) $T_1$. (e) $T_2$.

Fig. 3 shows the typical curves for the four parameters extracted from trajectory analysis (trajectory radius, speed, and two tortuosity indices) for three main movements: right, thorough and left turn (U-

turn was not considered due to the paucity of data examples). In the same Fig. 3, the cumulated values of these two indexes from the initial point at the entry gate ($i$ = 1) to the generic points ($i$) along the trajectory is also plotted.

The two indexes indicate the level of difficulty in negotiating the roundabout, which is higher when the angles are high and the corresponding radii are small. The units of measurement for the two tortuosity indexes are rad/m$^2$ and rad/m, respectively. In Fig. 3(d) and (e), they have been plotted according to the formulas with values that increase along the travelled path, for three trajectories selected from the Biella roundabout database (each identified with a 4-digit code). In Fig. 3(b) and (c), for the same three trajectories, the radius of the osculating circles and the speed profile are plotted. It is worth noting that in Fig. 3, the central point of the path has a reference station equal to 0.

As previously indicated, the speed at each of the $P_i$ points along a generic trajectory is calculated by simply dividing the distance between every point $P_i$ and the consecutive point $P_{i+1}$ by the elapsed time (equal to the frame rate of the video camera that was equal to 0.0333 s). For the radius diagram, thirty-one consecutive points of the trajectory (resulting in 1 s of images) have been considered for the estimation of $R_i$ values.

## 4 Investigation

With a view to establishing the optimal camera configuration and assessing the performance of VeTRA, in-field research activities were initially undertaken at five roundabouts in northern Italy (Piedmont and Lombardy regions), chosen for their geometrical characteristics and environment (rural and urban). Table 1 reports a synthesis of the geometric characteristics and the most significant survey data, while Fig. 4 illustrates three general video camera configurations used for the surveys.

Unfortunately, two other sites with different set-ups and in urban environment were investigated but recorded images were unusable due to the effects of a strong wind in one case and to a reflected dazzle in the latter that were not possible to remove.

Images were recorded for between 1.5 and 2 h to obtain at least one hour of actual flow. The recording period was in and around the peak hour of midday and, in all cases, the weather conditions were prevailingly dry and sunny with occasional passing clouds.

The first roundabout is located near the urban limits of the city of Biella (Fig. 5, with the identification of tracked vehicles, entry and exit gates, and video camera direction (arrow)), and connects two arterials with two lanes per direction and separated carriageways.

Pedestrian crossings are provided at three of the four legs. The external diameter is 50 m, the circulatory roadway is 13 m in width, while the central island diameter is equal to 24 m including a truck apron of 1.5 m. The approaching legs have two lanes with an average width of 8 m, while 6 m is the width of the single lane departure legs. The roundabout is equipped with a lighting tower headlight, while the water harvesting systems are located outside the circulatory roadway. During the study, the detection system was placed on a moveable rack near the edge of the southwest corner. The video camera, pointing towards the centre of the roundabout, was placed at a height of about 22 m at an angle of approximately 55° with respect to the rack axis.

**Table 1** Synthesis of information for survey activities.

| Roundabout | Biella | Ghisalba | Poncarale |
|---|---|---|---|
| Latitude | 45°33'12".39 | 45°35'32".21 | 45°27'29".99 |
| Longitude | 8°04'21".85 | 9°46'19".75 | 10°12'09".66 |
| Inscribed diameter, $D_{INS}$ (m) | 50 | 46 | 70 |
| Inner island diameter, $D_{INT}$ (m) | 24 | 26 | 56 |
| Circulatory roadway width, $W_{CR}$ (m) | 13 | 10 | 7 |
| Number of legs | 4 | 4 | 4 |
| Configuration # (Fig. 4) | 1 | 2 | 3 |
| Number of cameras | 1 | 3 | 3 |
| Manufacturer | Goyo GM12314S | No.2 Goyo GM12314S (2.30 mm, 94°) | Goyo GM12314S |
| (focal length, FOV) | (2.30 mm, 94°) | No.1 Theia MY125M (1.43 mm, 125°) | (2.30 mm, 94°) |
| Number of survey points | 1 | 1 | 2 |
| Video camera position | External | Internal | External |
| Horizontal angle (°) | - | 90 | 120 |
| Vertical angle (°) | 55 | 40 | 72 (1 camera)<br>55 (2 cameras) |
| Camera height (m) | 22 | 22 | 32 |

Note: FOV is field of view.

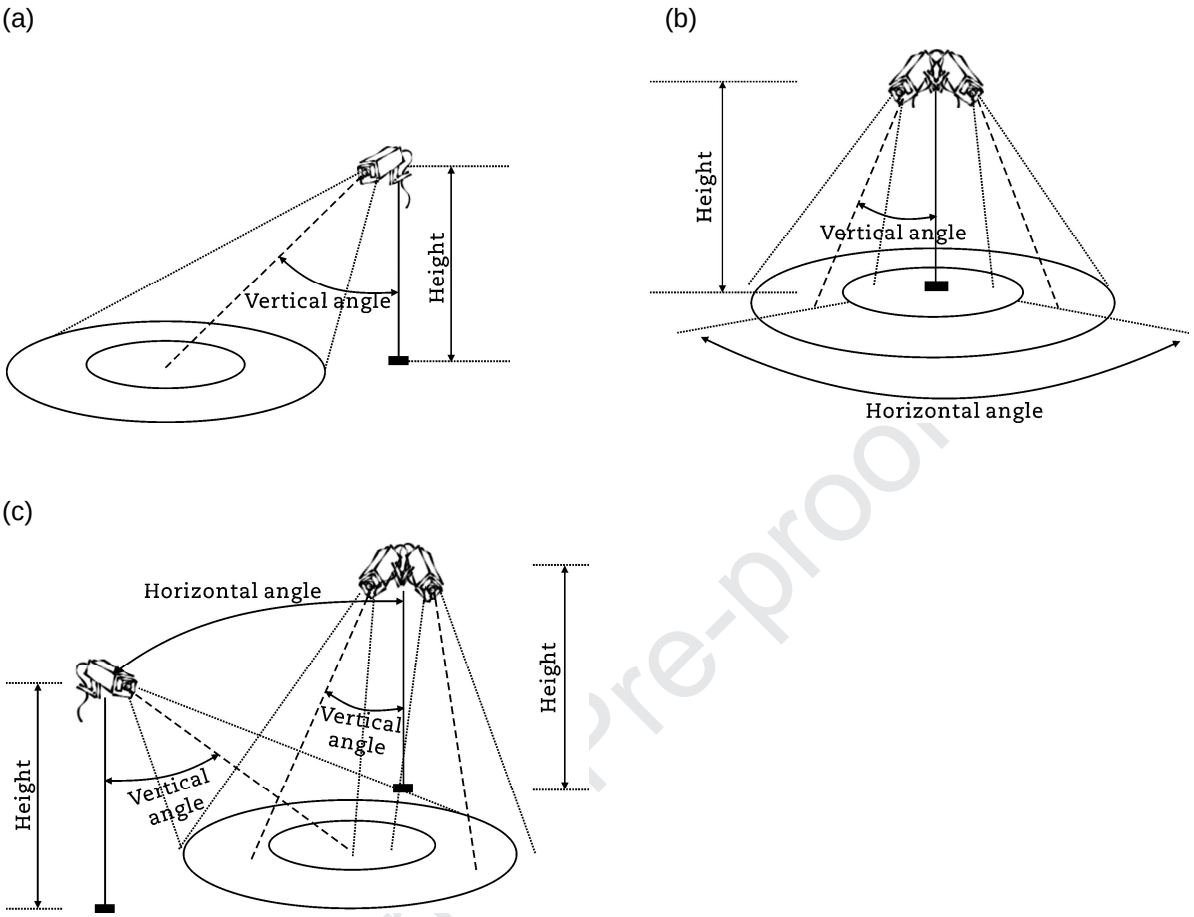


**Fig. 4** Scheme of the three video camera configurations adopted for the survey. (a) Configuration #1. (b) Configuration #2. (c) Configuration #3.

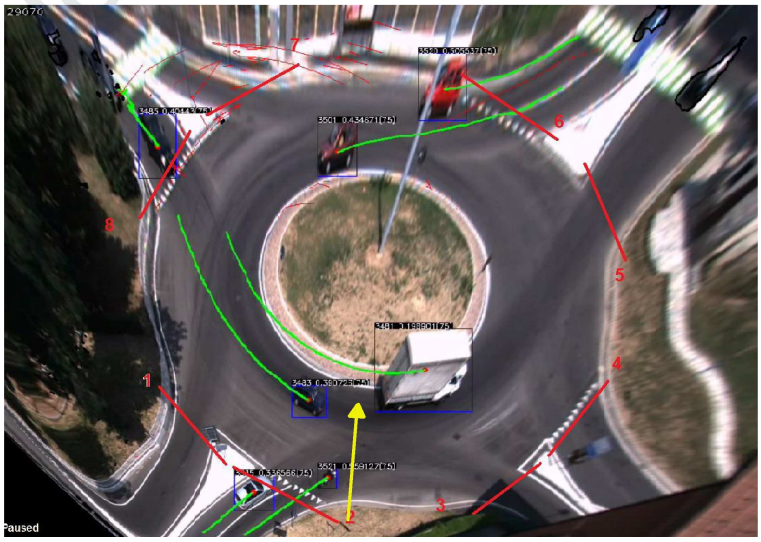

**Fig. 5** Aerial view of the Biella roundabout.

.

The second roundabout is located in a rural area near Ghisalba (Fig. 6(a)) at the intersection of two single-carriageway rural highways with no pedestrian crossings. The external diameter is 46 m, the circulatory roadway is 10 m, and the central island diameter is equal to 26 m with a truck apron of 2 m. The roundabout is furnished with a central lighting tower headlight. The detection system, consisting of three cameras, was placed on the lighting pole in the centre of the central island at a height of about 21 m above the roundabout plane, with the three cameras facing east, north and west respectively and placed at vertical angles of approximately 40° with respect to the pole.

The third roundabout lies outside the urban area of Poncarale (Fig. 6(b)) at the intersection of two main highways, both of which are single carriageway with two-way traffic and no pedestrian crossings. The external diameter is equal to 70 m and the circulatory roadway is only 7 m. As a result, the roundabout has a wide central island (56 m in diameter) that includes a truck apron of 2.5 m. In contrast with the other two roundabouts, the approaching and departure legs of the Poncarale roundabout are tangent to the circulatory roadway. The lighting is provided by two lighting towers, located on two divisional islands to the north and south, distant 81 and 28 m respectively from the roundabout.

(a) (b)

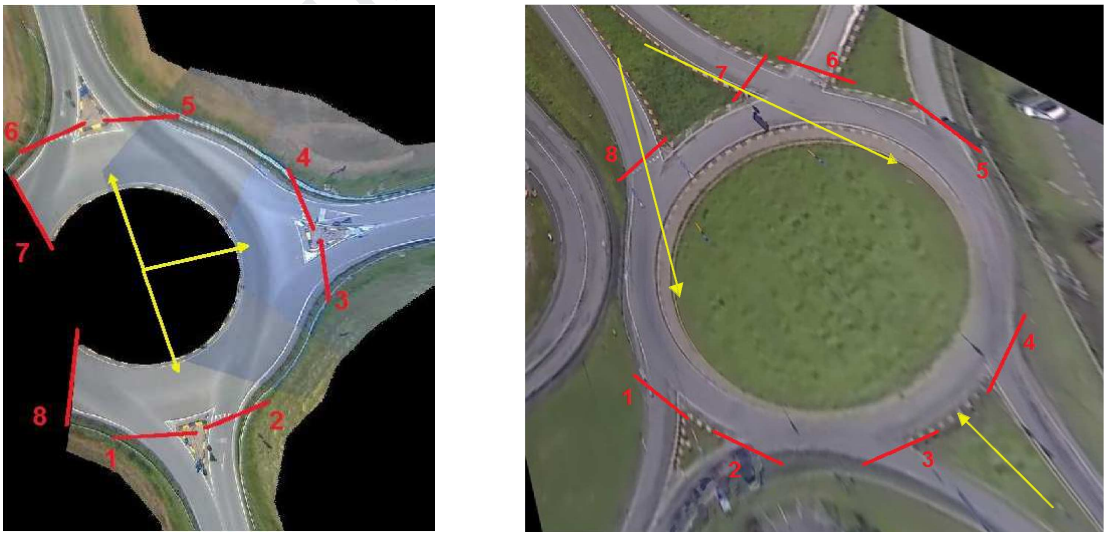


**Fig. 6** Aerial view of roundabouts. (a) Ghisalba roundabout. (b) Poncarale roundabout. (Arrows indicate video-camera direction).

The measurements were taken with three cameras installed at a height of 32 m, two of which were located on the southern lighting pole at an angle of approximately 55° and the third on the northern

lighting pole at an angle of approximately 72°. The cameras were attached to the lifting system to which the lamps of the central pole are fixed. This system is lifted and lowered whenever lamp maintenance is conducted. Since the video cameras were close to the lamps, it is reasonable to assume that they were not seen by drivers and so did not influence their behaviour. Survey vantage points were determined according to the particular set-up adopted (Fig. 4), with video cameras able to cover the entire roundabout.

## 5 Results and analysis

### *5.1 Vehicle classification and O/D matrix*

As explained before, the classification of vehicles has been limited to two classes of vehicles (light and heavy) which, when combined, represent more than 95% of the total observed flow for the three investigated case studies. Classification is worked out by a neural network previously trained through a sample of cases which are manually extracted.

Using different combinations of the two strategies cited previously (merged trajectories (MT) and blended images (BI)), the number of video cameras (from one to three (1C–3C)) and configurations (from #1 to #3), five different cases have been considered and reported in Table 2 to validate the estimates produced by VeTRA. In Table 2, the results are shown for all the possible sixteen movements into a 4-leg roundabout, with the last row containing the total number of movements recorded by VeTRA and the corresponding average values counted by the operators (specifically, three people who manually counted vehicles looking at the videos and subdividing such counts by movements).

The data elaborated by VeTRA and expressed in percentage terms ($v_i$), calculated on the total collected flow, were compared with those obtained from video observation by a number of operators. These measurements are reported in Table 2 in percentage under the column “Operator” ($o_i$), and were repeated until the average values between observations were significantly stable (i.e., the mean did not change anymore with the addition of new observations, according to the central limit theorem), and could be considered a “true” reference. Assuming application of the central limit theorem,

repeated extractions (analysis of same video images by the same operator) lead to a reduction in error when estimating the mean. It should be noted that the total number of vehicles observed in one hour of survey time was high (1500–2500 veh/h).

**Table 2** Comparison of percentage values of the O/D matrixes for Biella, Ghisalba and Poncarale roundabouts.

| O/D movement | Biella (configuration #1) | | Ghisalba (configuration #2) | | | Poncarale (configuration #3) | | |
|---|---|---|---|---|---|---|---|---|
| | Operator | VeTRA (%) | Operator | VeTRA (%) | | Operator | VeTRA (%) | |
| | (%) | 1C | (%) | 3C-MT | 3C-BI | (%) | 1C | 2C-BI |
| 2-1 | 0.40 | 0.59 | 0.00 | 0.00 | 0.00 | 0.14 | 0.00 | 0.10 |
| 2-3 | 2.93 | 3.37 | 2.98 | 4.72 | 3.56 | 7.14 | 4.70 | 12.02 |
| 2-5 | 20.96 | 20.33 | 26.46 | 23.29 | 25.89 | 7.24 | 3.65 | 0.10 |
| 2-7 | 0.47 | 0.44 | 1.08 | 1.15 | 1.47 | 3.48 | 1.05 | 6.11 |
| 4-1 | 3.26 | 2.49 | 0.00 | 0.00 | 0.00 | 5.43 | 5.89 | 7.46 |
| 4-3 | 0.20 | 0.26 | 0.00 | 0.10 | 0.05 | 0.28 | 0.07 | 0.10 |
| 4-5 | 4.64 | 4.80 | 0.66 | 1.20 | 0.95 | 4.64 | 7.36 | 0.10 |
| 4-7 | 7.82 | 6.87 | 2.53 | 2.45 | 2.61 | 17.76 | 18.58 | 30.05 |
| 6-1 | 19.79 | 21.13 | 0.00 | 0.00 | 0.00 | 9.60 | 12.90 | 0.00 |
| 6-3 | 4.66 | 2.60 | 0.00 | 0.14 | 0.00 | 4.08 | 4.84 | 0.00 |
| 6-5 | 0.29 | 0.00 | 0.00 | 0.05 | 0.00 | 0.09 | 0.07 | 0.00 |
| 6-7 | 7.07 | 8.68 | 31.22 | 30.46 | 29.98 | 0.19 | 0.84 | 0.21 |
| 8-1 | 2.05 | 2.71 | 30.60 | 31.95 | 31.54 | 7.79 | 8.27 | 9.12 |
| 8-3 | 11.90 | 13.27 | 2.03 | 2.26 | 2.19 | 19.67 | 27.70 | 34.09 |
| 8-5 | 13.22 | 12.24 | 2.40 | 2.17 | 1.71 | 12.29 | 3.86 | 0.00 |
| 8-7 | 0.33 | 0.23 | 0.04 | 0.05 | 0.05 | 0.19 | 0.21 | 0.52 |
| Total flow (veh) | 2002 | 2060 | 2415 | 2078 | 2105 | 2156 | 1706 | 1154 |

In this phase, the authors focused mainly on error evaluation rather than on absolute values, so Table 2 reports the percentage values for each movement with respect to the total number of movements.

Bernardin and Stiefelhagen (2008) suggested the use of clear multiple object tracking (MOT) metrics to measure the performance of video image processing. It is made up of two indexes: (a) the total error value averaged by the number of matches made when estimating position (indicated as MOTP–multiple object tracking precision–and discussed in the next subparagraph), and (b) the tracking accuracy (MOTA–multiple object tracking accuracy), estimated using the following equation.

$$\mathrm{MOTA} = 1 - \left(\sum_t (m_t + \mathrm{fp}_t + \mathrm{mmc}_t)\right) / \left(\sum_t g_t\right) \quad (6)$$

where for any time $t$, $m_t$ is the number of misses, $\mathrm{fp}_t$ is the number of false positives, $\mathrm{mmc}_t$ is the number of mismatches, and $g_t$ is the number of objects.

In this application, we calculated MOTA using all data collected by operator but only data for completely detected trajectories by VeTRA (since partially revealed trajectories are not of interest in this context and then the number of objects, $g$, is lower), thus leading to possible worse performance. Therefore, the subscript $t$ (usually the index of each frame) is here assumed to be linked to a whole trajectory. This index varies from 1 to 0 (from best to worst performance). Besides, differences between operator and VeTRA are firstly calculated for each movement and then summed up. Three other different error types were also calculated from Table 2 and listed in Table 3 according to performance indexes used in technical literature: the sum of absolute differences ($E_1$), the average of absolute differences ($E_2$), and the average of differences ($E_3$). $E_1$, $E_2$, and $E_3$ are calculated according to the following equations.

$$E_1 = \sum_i |v_i - o_i| \tag{7}$$

$$E_2 = \sum_i |v_i - o_i| / n \tag{8}$$

$$E_3 = \sum_i (v_i - o_i) / n \tag{9}$$

where $n$ represents the number of movements considered in the analysis.

Difference between $E_1$ and $E_2$ depends only on the number of movements $n$ taken into consideration but this number may change from site to site. Hence, when comparing performance of two sites, it may be useful to use both indexes. Besides the indexes, their percentages were also taken into consideration. They were calculated considering $v_i / \sum_i v_i$ instead of $v_i$ for $E_1$, and $o_i / \sum_i o_i$ instead of $o_i$ for $E_2$. For $E_3$, the average percentage is always nil.

It must be stressed that operators represent the way to obtain the true result by application of the central limit theorem. In this experiment, since an infinite number of operators is not possible, the calculated averages may be considered a good estimate of the true result. VeTRA results are, nonetheless, affected by deterministic errors that cannot be completely avoided since they are intrinsic to the system (i.e., video cameras and lenses).

Values for the average of the absolute differences (Table 2) between operator and VeTRA generated data are less than 5% and are compatible with traffic analysis resolution. This also holds true, albeit to a lesser extent, for the average of percentage differences (considering all movements).

In contrast, the sum of percentage differences is generally very high even with the best strategy (see Ghisalba-BI and Biella-1C in Table 2).

This last result shows the existence of a bias due to the general set-up conditions during the survey. The fact that bias is positive indicates that VeTRA has generally estimated a lower percentage value for each movement than that obtained by the operators. In the cases of Biella and Poncarale, the bias is positive, while in Ghisalba, it is negative.

On examination of the five analyses carried out with VeTRA (Tables 2 and 3), the best results were obtained with configuration #1 in Fig. 4, in particular when considering the MOTA index. In fact, the performance obtained with the use of one video camera, which has lower costs and requires less effort, is quite similar to that of configuration #2 in which three video cameras are employed. Moreover, in the latter case at least four video cameras would be necessary to ensure adequate coverage of the entire surface of the roundabout (Fig. 6).

The problems resulting from the blending of sequences obtained from three video cameras located at 32 m from the roundabout (configuration #3 of Fig. 4) led to the necessity of considering two different strategies in the analysis of the Poncarale roundabout. Although the performance indicators (in Table 3) in the case of three-camera (Ghisalba-3C) and also a single camera (1C) configurations are still quite close to those established in the Biella case study, the use of a two-camera (2C) configuration with blended images results in the worst performance observed.

The use of additional cameras can result in operating problems related to factors such as synchronization between frames from different cameras, different orientations and separated communication wires. Synchronization is an acute problem that can be exacerbated by the loss of some frames. In addition, the different orientation of video cameras requires different isomorphisms, that is, different camera calibrations and homography transformations. The result obtained for $E_3$ of Biella, which is indeed very low, is not surprising since Eq. (9) does not use absolute values and therefore errors, which are not very biased in this case, cancel each other.

**Table 3** Performance indicators (errors) between operator and VeTRA computed values according to Eqs. (6)-(8).

| Roundabout and image treatment strategy | $E_1$ (sum of absolute differences) | | $E_2$ (average of absolute differences) | | $E_3$ (average of differences) | MOTA (%) |
|---|---|---|---|---|---|---|
| | Percentage (%) | Value (veh) | Percentage (%) | Value (veh) | Value (veh) | |
| Biella (1C) | 11.64 | 58 | 0.72 | 4 | 0.89 | 88 |
| Ghisalba (3C-MT) | 8.47 | 419 | 0.53 | 26 | 21.00 | 82 |
| Ghisalba (3C-BI) | 5.03 | 336 | 0.31 | 21 | 19.00 | 86 |
| Poncarale (1C) | 34.52 | 643 | 2.15 | 41 | 28.00 | 70 |
| Poncarale (2C-BI) | 75.88 | 1006 | 4.74 | 63 | 63.00 | 53 |

### *5.2 Positions and speeds validation*

Since the distances between the RTK-GPS data and the VeTRA probe vehicle obtained data are not Gaussian distributed, the MOTP index (Bernardin and Stiefelhagen, 2008) is split into three other indexes – the median, median of absolute deviations (MAD), and inter-quartile range (IQR) (Table 4).

The results are available for the six different analyses carried out on the three roundabouts and the different strategies of image processing. Furthermore, Table 4 lists the average and the standard deviation of the speed differences recorded by both the on-board RTK-GPS system and by the tracking process, for the same combination of roundabout and image processing strategies.

The results show that differences in positions and speed occur when different configurations and processing strategies are adopted. The best performances in terms of tracking were observed in the following cases: single camera configuration (Biella), two cameras with image blending (2C-BI) and merged trajectory (2C-MT) strategy (Poncarale). Greater distances between tracked points were measured when configuration #2 of Fig. 4 with three central cameras was adopted, and in the case of the survey carried out at Poncarale, where only one camera was used to analyse vehicle movements at a roundabout with the largest diameter (70 m) between the three here investigated.

As regards speeds, the best results in terms of average and standard deviation were noted in the Biella survey, while the worst performances were those in the Poncarale survey in which the image analysis procedure was conducted with one camera only. This would suggest the necessity to use more than one camera for surveys of roundabouts larger than the Poncarale one.

**Table 4** Distribution of errors in distance and speed difference between VeTRA and RTK-GPS data.

| Roundabout | Distance (m) | | | Speed difference (km/h) | |
|---|---|---|---|---|---|
| | Median | MAD | IQR | Average | Standard deviation |
| Biella (1C) | 0.375 | 0.179 | 0.399 | 0.11 | 2.71 |
| Ghisalba (3C-MT) | 0.651 | 0.457 | 0.863 | 0.12 | 7.31 |
| Ghisalba (3C-BI) | 0.272 | 0.743 | 0.619 | 3.06 | 8.87 |
| Poncarale (1C) | 0.576 | 0.250 | 0.576 | 11.46 | 23.66 |
| Poncarale (2C-MT) | 0.383 | 0.191 | 0.436 | 1.06 | 8.64 |
| Poncarale (2C-BI) | 0.384 | 0.173 | 0.397 | 7.58 | 18.71 |

In the case of Poncarale with the strategy 2C-MT, data analysis was limited to speed analysis and not extended to the whole set of analyses due to difficulties in building the whole trajectory. In too many cases, the continuity of the trajectory curve was not achieved.

### *5.3 Tortuosity and speeds analysis*

An analysis of tortuosity and related speeds was performed on the class of light vehicles only. For each trajectory and at each point ($i$), VeTRA derives the two tortuosity indexes and local speeds from the recorded positions and times when the centre of the vehicle occupies the points $i$+1, $i$ and $i$-1. All the trajectories are grouped under the same O/D maneuver and the software can elaborate the requested statistical output selected by the operator.

Table 5 contains the synthesis of the 15th percentile of the two tortuosity indexes ($T_{1,15}$ and $T_{2,15}$) calculated for those parts of the trajectories including the entry and exit gates of the roundabouts, and the 85th percentile of corresponding speeds at: (1) the entry gate ($V_{1,85}$), (2) the midpoint of the trajectory inside the circulatory roadway ($V_{2,85}$), and (3) the exit gate ($V_{3,85}$) as indicated in Fig. 1. The data in Table 5 was evaluated on the base of 2208 measurements of light vehicles operating in free-flow conditions. According to Fig. 6(a), in the case of Ghisalba, only three maneuvers were completely measured; in the case of Biella and Poncarale, the number of performance measures per O/D was lower than sixteen (four origins per four destinations) since the number of vehicles recorded for certain maneuvers (typically the U-turn) was too low.

**Table 5** Filtered trajectory data for 15th percentile of tortuosity and 85th percentile of operating speed.

| Roundabout | O/D | Maneuver | No. of data | $T_{1,15}$ (rad/m$^2$) | $T_{2,15}$ (rad/m) | $V_{1,85}$ (km/h) | $V_{2,85}$ (km/h) | $V_{3,85}$ (km/h) |
|---|---|---|---|---|---|---|---|---|

| | | | | | | | | |
|---|---|---|---|---|---|---|---|---|
| Biella 1C | 2-3 | Right turn | 20 | 0.00124 | 0.0311 | 32.27 | 34.07 | 39.37 |
| | 2-5 | Crossing | 185 | 0.00015 | 0.0096 | 33.88 | 39.00 | 44.11 |
| | 4-1 | Left turn | 21 | 0.00200 | 0.0372 | 29.58 | 27.75 | 40.55 |
| | 4-5 | Right turn | 50 | 0.00129 | 0.0330 | 29.33 | 30.44 | 33.62 |
| | 4-7 | Crossing | 73 | 0.00069 | 0.0216 | 30.61 | 36.09 | 41.38 |
| | 6-1 | Crossing | 185 | 0.00094 | 0.0255 | 32.71 | 33.43 | 42.68 |
| | 6-3 | Left turn | 42 | 0.00207 | 0.0383 | 33.70 | 29.52 | 42.43 |
| | 6-7 | Right turn | 83 | 0.00064 | 0.0218 | 34.63 | 34.66 | 37.27 |
| | 8-1 | Right turn | 20 | 0.00054 | 0.0207 | 31.89 | 33.08 | 37.88 |
| | 8-3 | Crossing | 72 | 0.00041 | 0.0163 | 36.11 | 35.51 | 44.56 |
| | 8-5 | Left turn | 97 | 0.00179 | 0.0336 | 33.56 | 27.81 | 39.64 |
| Ghisalba 3C-BI | 2-3 | Right turn | 33 | 0.00047 | 0.0204 | 34.15 | 36.27 | 35.52 |
| | 2-5 | Crossing | 364 | 0.00070 | 0.0224 | 36.70 | 35.80 | 40.07 |
| | 4-5 | Right turn | 9 | 0.00032 | 0.0168 | 35.25 | 38.66 | 40.76 |
| Ghisalba 3C-MT | 2-3 | Right turn | 33 | 0.00050 | 0.0203 | 30.70 | 32.90 | 33.67 |
| | 2-5 | Crossing | 364 | 0.00067 | 0.0221 | 36.41 | 35.83 | 40.22 |
| | 4-5 | Right turn | 9 | 0.00037 | 0.0182 | 31.57 | 34.61 | 39.18 |
| Poncarale 2C-BI | 4-1 | Left turn | 42 | 0.00077 | 0.0241 | 43.60 | 37.70 | 47.02 |
| | 4-7 | Crossing | 183 | 0.00035 | 0.0152 | 40.26 | 39.59 | 46.31 |
| | 2-3 | Right turn | 22 | 0.00100 | 0.0298 | 32.43 | 32.71 | 38.91 |
| | 2-7 | Left turn | 28 | 0.00075 | 0.0233 | 34.67 | 35.47 | 44.92 |
| | 8-3 | Crossing | 226 | 0.00048 | 0.0177 | 37.76 | 38.03 | 45.25 |
| | 8-1 | Right turn | 47 | 0.00007 | 0.0065 | 39.09 | 44.88 | 49.48 |

The 85th percentile of speed distribution is widely considered in the geometric design of highways. It is compared with the design speed to assess speed consistency between the hypothesis of designer and driver behaviour. It reflects the movement of isolated vehicles (i.e., free-flow conditions), and separates the population of prudent drivers from the group of more aggressive ones (Yasser and Mohamed, 2011).

The choice of the two percentiles is based on the supposition that aggressive drivers, whose speeds exceed the 85th percentile, tend to follow the fastest path that should be characterized by the lowest tortuosity (as also suggested in Rodegerdts et al., 2007, 2010). The authors associated the 15th percentile of tortuosity indexes with the fastest path so as to establish correlations between trajectory and speeds.

When the analysis is confined to a part of the speed data, the most significant relationships between the values reported in Table 5 are limited to the 85th percentile of speeds calculated at the

middle point of trajectories ($V_{2,85}$) and the 15th percentile of the two tortuosity indexes $T_{1,15}$ and $T_{2,15}$. The results are reported in Figs. 7 and 8, and demonstrate that $T_{2,15}$ rather than $T_{1,15}$ has a rather good correlation to $V_{2,85}$ as confirmed by the statistics of the two models summarized in Table 6.

Figs. 7 and 8 also report the data generated with the MT strategy in the case of the Ghisalba roundabout. These data are more dispersed when compared to the corresponding data derived with the BI strategy, and, as a consequence, they were not taken into account in the exponential model which was plotted in both figures, and which exhibited the highest coefficient of determination for both tortuosity indexes.

Very low correlation values were found between the 85th percentile of entry ($V_1$) and exit ($V_3$) speeds. This may be attributed to the fact that the entry speed largely depends on driver behaviour in the approaching leg, while the exiting speed depends more on the specific shape of curbs around the exit lane.

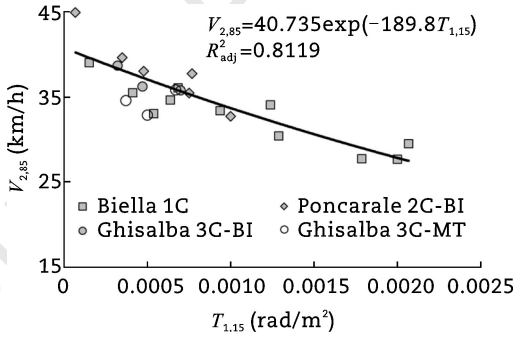


**Fig. 7** Relationship between $V_{2,85}$ and $T_{1,15}$ index.

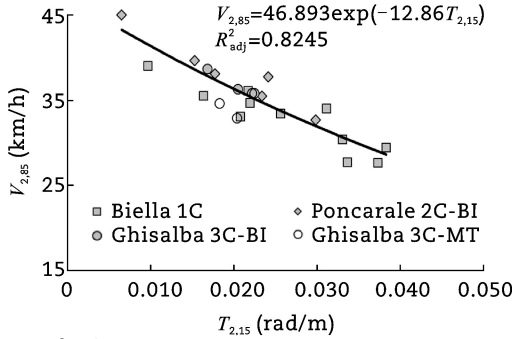


**Fig. 8** Relationship between $V_{2,85}$ and $T_{2,15}$ index.

**Table 6** Output of statistics for model reported in Figs. 7 and 8.

| Model | $V_{2,85}$ = 40.735exp (−189.8$T_{1,15}$) | $V_{2,85}$ = 46.893exp (−12.86$T_{2,15}$) |
|---|---|---|

| | | | |
|---|---|---|---|
| $R^2$ | | 0.8218 | 0.8337 |
| $R^2$ adjusted | | 0.8119 | 0.8245 |
| Standard error | | 0.0520 | 0.0510 |
| $F$ value | | 83.0259 | 90.2644 |
| | | ($F$ critical = 2.17, $p$ = 0.05) | ($F$ critical = 2.17, $p$ = 0.05) |
| $p$ value | Intercept | $1.27\times10^{-30}$ | $2.90\times10^{-27}$ |
| | Variable | $3.66\times10^{-8}$ | $1.95\times10^{-8}$ |

618

619 It must be stressed that we limited the study of correlation between speed and tortuosity only to
620 three points (entry, middle and exit) as reproduction of the approach proposed by Rodegerdts et al.
621 (2007).

622 *5.4 Acceleration analysis*

623 Table 7 shows the statistics for acceleration and deceleration measured on the circulatory roadway for
624 the Ghisalba and Poncarale roundabouts (trajectory data are the same of Table 5). It should be
625 highlighted once again that the data considered here pertain to vehicles that were not affected by
626 other vehicles when negotiating the roundabout, thus all the data can be considered to be that of
627 isolated vehicles and drivers affected by the roundabout geometrics only.

628 According to the speed variation model depicted in Fig. 1, the deceleration from sections 1 to 2 is
629 indicated as $a_{12}$, while the acceleration from the central point of the trajectory (section 2) to the exit
630 section (section 3) is indicated as $a_{23}$.

631 **Table 7** Statistics for vehicular acceleration and deceleration at the Ghisalba and Poncarale roundabouts.
632

| Roundabout | Ghisalba 3C-BI | | | | Poncarale 2C-BI | | | | | |
|---|---|---|---|---|---|---|---|---|---|---|
| | Right turn | | Through | | Right turn | | Through | | Left turn | |
| Acceleration | $a_{12}$ | $a_{23}$ | $a_{12}$ | $a_{23}$ | $a_{12}$ | $a_{23}$ | $a_{12}$ | $a_{23}$ | $a_{12}$ | $a_{23}$ |
| No. of objects | 42 | 42 | 364 | 364 | 69 | 69 | 409 | 409 | 70 | 70 |
| Mean (m/s$^2$) | −0.614 | 0.116 | −0.063 | 0.409 | −0.674 | 0.719 | −0.264 | 0.468 | −0.051 | 0.358 |
| Standard deviation (m/s$^2$) | 0.601 | 0.499 | 0.370 | 0.273 | 1.030 | 0.660 | 0.555 | 0.616 | 0.312 | 0.204 |
| 15th percentile (m/s$^2$) | −1.241 | −0.556 | −0.378 | 0.142 | −1.724 | 0.117 | −0.831 | 0.141 | −0.371 | 0.205 |
| 85th percentile (m/s$^2$) | −0.038 | 0.606 | 0.281 | 0.676 | 0.132 | 1.261 | 0.235 | 0.744 | 0.257 | 0.543 |
| Max (m/s$^2$) | 0.213 | 1.075 | 1.160 | 1.204 | 3.037 | 2.796 | 2.228 | 11.141 | 0.838 | 0.739 |

| | | | | | | | | | | |
|---|---|---|---|---|---|---|---|---|---|---|
| Min (m/s$^2$) | −1.901 | −0.721 | −1.948 | −0.793 | −3.201 | −1.474 | −2.156 | −0.832 | −0.895 | −0.518 |

Per each vehicle traversing the roundabout, these two values were computed with the following equations.

$$a_{12} = (v_{22} - v_{12}) \,/\, (2d_{12}) \tag{10}$$

$$a_{23} = (v_{32} - v_{22}) \,/\, (2d_{23}) \tag{11}$$

where $d_{12}$ and $d_{23}$ have the same meaning of Eqs. (1) and (2). Data have also been distinguished for left turn, right turn, and through movements.

The mean and the standard deviation of acceleration values indicate that entering vehicles in deceleration ($a_{12}$) and exiting vehicles in acceleration ($a_{23}$) exhibit large variations as a result of the roundabout layout and geometrics, and type of maneuvers. The 15th percentiles of deceleration ($a_{12}$), listed in Table 7, are only higher in the case of right turn movements than the absolute value of 1.3 m/s$^2$ suggested in Rodegerdts et al. (2007), and reflect the behaviour of aggressive drivers. In all other cases, the statistics for $a_{12}$ indicate that lower values are observed.

Regarding the acceleration variable ($a_{23}$), a large difference is evident between the observed values and the value of 2.3 m/s$^2$ proposed again in Rodegerdts et al. (2007), thus suggesting the need for an extended investigation into a greater number of roundabout geometry types. In fact, the two roundabouts considered here yield different results as a consequence of the significant difference in their layout.

## 6 Discussion

The results illustrated in previous paragraphs outlined the strengths and weaknesses associated with each set-up for the three different roundabouts considered in the investigation. In the three cases, small camera oscillations, clouds, and flying objects (i.e., birds) affecting image quality were easily identified and corrected.

On examination of the three configurations presented in Fig. 4, it is clear that the central position of the video cameras facilitates a reduction in perspective distortion but, as in the case of Ghisalba (configuration #2 in Fig. 4 with three cameras), a relatively high number of video cameras is required

given the dimensions of the circulatory roadway. The blending of images becomes more complicated with an increase in the number of video cameras installed at or around the roundabout. Moreover, synchronization between cameras becomes crucial: with the loss of only one frame of a video camera necessitating a challenging task of realignment between video frames.

Elevated vantage points on poles or buildings introduce high levels of distortion especially in the case of heavy and long vehicles, as in the case of Poncarale (configuration #3 in Fig. 4 with three cameras). Furthermore, the height of vantage points has a detrimental impact on image quality since the cameras and their supports are exposed to stronger winds, which can produce oscillations that are hard to correct during the image treatment phase. From an analysis of the data collected at the Poncarale roundabout, it would appear that the merging of trajectories extracted from different images (MT strategy) seems to be less effective than the blending images (BI) technique. In this case, the only one for which this comparison has been made, the performance indicators associated with the evaluation of the O/D matrix indicate a greater dispersion of data in the case of the merged trajectory technique (Table 5).

Whereas the blending of images is essentially a straightforward task when video cameras have viewing angles of less than 90°, it tends to prove problematic with wider angles (especially those closer to 180°) as a consequence of the different perspective distortions of moving elements. Of the three configurations considered in this research, the use of a single video camera mounted on a pole located outside the roundabout, as in the case of Biella (with the camera located at the external side of the circulatory roadway), would appear to offer the best compromise in terms of survey costs, pre-processing work, and quality of results. However, this is not a definitive conclusion, since the number of experiments carried out to date is not considered comprehensive from a technological point of view. In this study, the authors focused primarily on a general evaluation of the methodology and the estimation of technical problems to be solved for each specific configuration. In fact, while the results here have been used to assess the survey methodology, they cannot be considered statistically significant in terms of the performances of the investigated roundabouts or, indeed, roundabouts in general.

In all the three configurations depicted in Fig. 4, VeTRA has been able to collect spatial and temporal data for a large number of points along each trajectory, thus deriving local speeds. The authors decided to consider speeds at the entry gate, at the midpoint and at the exit of the roundabout to compare results with those in Rodegerdts et al. (2007). Two different tortuosity indexes were calculated for each trajectory by combining angular deviation and the distance between two successive recorded points, and the radius of the local osculating circle in different ways.

As a result, some linear and exponential relationships between the 85th percentile of speeds and the 15th percentile of tortuosity indexes have been derived. The observations confirm that an effective speed control within the circulatory roadway is possible only when high horizontal curvatures of vehicle paths (i.e., high values of tortuosity) are achieved as a consequence of the combination of the geometric characteristics of roundabout elements.

The regression equations presented here were obtained from 2208 speed data (Table 5) of just three roundabouts with each exhibiting a different geometry in terms of external and central island diameters, circulatory roadway width, number and geometry of entry and exit lanes. The high coefficient of determination of one of the four proposed equations ($R^2$ = 0.8337 for the exponential relationship between $V_{2,85}$ and the $T_{2,15}$) facilitates its use in the estimation of the circulating operating speed ($V_{2,85}$) in the analysis and design of roundabouts.

Acceleration and deceleration values on the circulatory roadways exhibit large variations as a consequence of roundabout layout and geometrics, maneuver type, and driving attitudes and styles. In light of the observation data, the suggested values of −1.3 m/s$^2$ in deceleration and 2.1 m/s$^2$ in acceleration included in the NCHRP Reports 572 and 672 (Rodegerdts et al., 2007, 2010) seem to be questionable, thus new research is necessary to obtain better design-operating speed and acceleration distribution on the circulatory roadway. This paper has demonstrated that image analysis has the potential to achieve such objectives.

## 7 Conclusions

The paper presents the results of several activities undertaken involving extensive use of the VeTRA software and acquisition tools, which the authors developed for the specific purpose of carrying out operational analyses of roundabouts through the use of video-tracking technology.

At present, the comprehensive gathering of operational data at roundabouts necessitates the use of non-integrated acquisition systems and prolonged data analysis times. Since 2010, the authors have worked on the development of an integrated system (specifically designed for roundabouts) composed of a hardware system for data acquisition and collection, and software for data analysis.

The system and some data analysis have already been presented in previous referenced works (Mussone et al., 2011, 2013), in which the system included one video camera only.

In this paper, the authors focused their attention on an extended use of the software with the aims of solving issues related to the survey configuration used with more than one video camera and their positioning inside or around the roundabout, and improving the tracking system of vehicles and deriving the O/D matrix and trajectories (i.e., position and time of tracked vehicles).

Two possible strategies consisting in (a) the merging of trajectories extracted from each separate video, and (b) the image blending from different video cameras before extracting trajectories were investigated. Results suggest that the second is more effective than the first one. Furthermore, of the three configurations considered, the one consisting in a single video camera mounted on a pole outside the roundabout appeared to be the optimal in terms of costs, processing work, and quality of results. However, this solution may imply large perspective distortion of the tracked vehicles in locations far from the camera, especially in case of roundabout with large diameters. To limit perspective distortion, the vantage point must be raised up as much as possible.

From the data collected from case studies, one further result concerns the correlation between speed and tortuosity of vehicle trajectories, which could be used by designers in the estimation of vehicle performance when negotiating a roundabout. This result emphasizes the tremendous potential of the image analysis in capturing position and kinematic of vehicles, and opens up to further studies on the evaluation of the operational effects of roundabouts.

In conclusion, previous works by the authors, together with the results reported in this paper, testify to the fact that the video survey system and the processing code are both robust and reliable. As documented in this paper, the authors are aware that further work is necessary to improve the performance of the tracking system of VeTRA in all possible set-up configurations.

With this objective in mind, a new version of the software is under development. It will include a set of 3D models of vehicles that differ in terms of dimensions and that can be associated with each blob. In this way, trajectories will be derived with reference to the geometric centre of the model rather than to the centre of the blob. This approach, already adopted by some authors but in different road scenarios (Kim et al., 2005; Koller et al., 1993; Messelodi et al., 2005), can lead to better vehicle recognition, which is considerable when high perspective distortions are present (like in Poncarale), together with even more precise localization and tracking. The authors are confident that the use of vehicle models will reduce the negative effect of video camera oscillations and will enable the separation of the shadows (of vehicles) from the actual vehicles in blobs, thus reducing the impact of shadows on the quality of collected data. Finally, to extend the possibility of data collection to night-time conditions, new research will also be carried out assessing how to use videos from thermal and/or infra-red video cameras.

## Conflict of interest

The authors do not have any conflict of interest with other entities or researchers.

## References

Ahac, S., Džambas, T., Dragčević, V., 2016. Review of fastest path procedures for single-lane roundabouts. In: The 4th International Conference on Road and Rail Infrastructure (CETRA), Sibenik, 2016.

Alhajyaseen, W.K.M., Asano, M., Nakamura, H., et al., 2013. Stochastic approach for modeling the effects of intersection geometry on turning vehicle paths. Transportation Research Part C: Emerging Technologies 32, 179-192.

765 Apeltauer, J., Babinec, A., Herman, D., et al., 2015. Automatic vehicle trajectory extraction for traffic
766 analysis from aerial video data. The International Archives of Photogrammetry, Remote Sensing
767 and Spatial Information Sciences 40(3), 9.
768 Autodesk, 2018. Civil 3D: Civil Infrastructure Design and Documentation Software. Available at:
769 https://www.autodesk.com/products/civil-3d/overview (Accessed 10 September 2019).
770 Bernardin, K., Stiefelhagen, R., 2008. Evaluating multiple object tracking performance: the CLEAR
771 MOT metrics. EURASIP Journal on Image and Video Processing 2008, 1-10.
772 Beymer, D., McLauchlan, P., Coifman, B., et al., 1997. A real-time computer vision system for
773 measuring traffic parameters. In: IEEE Computer Society Conference on Computer Vision and
774 Pattern Recognition, San Juan, 1997.
775 Curti, V., Marescotti, L., Mussone, L., 2008. Roundabouts: Design and Evaluations of Roundabout
776 Intersections, fourth ed. Maggioli, Ravenna.
777 Datondji, S.R.E., Dupuis, Y., Subirats, P., et al., 2016. A survey of vision-based traffic monitoring of
778 road intersections. IEEE Transactions on Intelligent Transportation Systems 17(10), 2681-2698.
779 Dinh, H., Tang, H., 2017. A video processing system for automated traffic data collection of gap size
780 for roundabouts. In: IEEE 30th Canadian Conference on Electrical and Computer Engineering,
781 Windsor, 2017.
782 Fernandes, P., Salamati, K., Rouphail, N.M., et al., 2015. Identification of emission hotspots in
783 roundabouts corridors. Transportation Research Part D: Transport and Environment 37, 48-64.
784 Grenard, J.L., Wei, T., 2012. Traffic Counting at Roundabouts Using Video Technology: A
785 Practitioner's View–White Paper. Available at: http://miovision.com/white-papers-research-reports/
786 (Accessed 2 March 2014).
787 Guido, G., Gallelli, V., Rogano, D., et al., 2016. Evaluating the accuracy of vehicle tracking data
788 obtained from unmanned aerial vehicles. International Journal of Transportation Science and
789 Technology 5(3), 136-151.
790 Kim, Z.W., Gomes, G., Hranac, R., et al., 2005. A machine vision system for generating vehicle
791 trajectories over extended freeway segments. In: 12th World Congress on Intelligent
792 Transportation Systems, San Francisco, 2005.

Koller, D., Daniilidis, K., Nagel, H.H., 1993. Model-based object tracking in monocular image sequences of road traffic scenes. International Journal of Computer Vision 10(3), 257–281.

Messelodi, S., Modena, C.M., Zanin, M., 2005. A computer vision system for the detection and classification of vehicles at urban road intersections. Pattern Analysis and Applications 8(1-2), 17-31.

Migliore, D.A., Matteucci, M., Naccari, M., 2006. A revaluation of frame difference in fast and robust motion detection. In: The 4th ACM International Workshop on Video Surveillance and Sensor Networks, Santa Barbara, 2006.

Mussone, L., 2013. The analysis of roundabouts through visibility. Procedia – Social and Behavioral Sciences 87, 250-268.

Mussone, L., Matteucci, M., Bassani, M., et al., 2011. Traffic analysis in roundabout intersections by image processing. In: The 18th International Federation of Automatic Control (IFAC) World Congress, Milano, 2011.

Mussone, L., Matteucci, M., Bassani, M., et al., 2013. An innovative method for the analysis of vehicle movements in roundabouts based on image processing. Journal of Advanced Transportation 47(6), 581–594.

Oh, J., Min, J., Heo, B., 2012. Development of an integrated system based vehicle tracking algorithm with shadow removal and occlusion handling methods. Journal of Advanced Transportation 46(2), 139–150.

Perco, P., Marchionna, A., Falconetti, N., 2012. Prediction of the operating speed profile approaching and departing intersections. Journal of Transportation Engineering 138(12), 1476-1483.

Robinson, B.W., Rodegerdts, L., Scarbrough, W., et al., 2000. Roundabouts: an Informational Guide. FHWA-RD-00-067. Federal Highway Administration, U.S. Department of Transportation, Washington DC.

Rodegerdts, L., Blogg, M., Wemple, E., et al., 2006. Appendixes to NCHRP Report 572: Roundabouts in the United States. NCHRP Web-Only Document 94. Transportation Research Board, National Research Council, Washington DC.

Rodegerdts, L., Blogg, M., Wemple, E., et al., 2007. Roundabouts in the United States. NCHRP Report 572. Transportation Research Board, National Research Council, Washington DC.

Rodegerdts, L., Bansen, J., Tiesler, C., et al., 2010. Roundabouts: an Informational Guide. NCHRP Report 672. Transportation Research Board, National Research Council, Washington DC.

Rodegerdts, L., Jenior, P.M., Bugg, Z.H., et al., 2014. Evaluating the Performance of Corridors with Roundabouts. NCHRP Report 772. Transportation Research Board, Washington DC.

Sacchi, E., Bassani, M., Persaud, B., 2011. Comparison of safety performance models for urban roundabouts in italy and other countries. Transportation Research Record 2265, 253-259.

Sakshaug, L., Laureshyn, A., Svensson Å., et al., 2010. Cyclists in roundabouts – different design solutions. Accident Analysis & Prevention 42(4), 1338-1351.

Salamati, K., Coelho, M.C., Fernandes, P., et al., 2013. Emissions estimation at multilane roundabouts: effects of movement and approach lane. Transportation Research Record 2389, 12-21.

St-Aubin, P., Saunier, N., Miranda-Moreno, L.F., 2013. Detailed driver behaviour analysis and trajectory interpretation at roundabouts using computer vision data. Transportation Research Record 2389, 65-77.

Šurdonja, S., Dragčević, V., Deluka-Tibljaš, A., 2018. Analyses of maximum-speed path definition at single-lane roundabouts. Journal of Traffic and Transportation Engineering (English Edition) 5(2), 83-95.

Suzuki, K., Nakamura, H., 2006. TrafficAnalyzer – the integrated video image processing system for traffic flow analysis. In: The 13th Intelligent Transportation Systems World Congress, London, 2006.

Transoftsolutions, 2018. TORUS Roundabouts: Roundabout Design Software. Available at: https://www.transoftsolutions.com/road-design/torus-roundabouts/ (Accessed 2 January 2019).

Wei, H., Feng, C., Meyer, E., et al., 2005. Video-capture-based approach to extract multiple vehicular trajectory data for traffic modeling. Journal of Transportation Engineering 131(7), 496-505.

Yasser, H., Mohamed, S., 2011. Modeling Operating Speed. Transportation Research Circular Synthesis Report E-C151. Transportation Research Board, Washington DC.

Zaki, M.H., Sayed, T., Cheung, A., 2013. Computer vision techniques for the automated collection of cyclist data. Transportation Research Record 2387, 10-19.

Marco Bassani, PhD, is an associate professor in roads, railways and airport engineering at the Politecnico di Torino (Italy) where he teaches “Design of Transportation Infrastructures”. In 2014, he was a visiting professor at the University of Maryland (College Park, US). His main research interests and publications are related to the use of alternative materials, advanced geometric design of roads, driving simulation, and road safety. Since 2016, he is in the editorial board of Transportation Letters: The International Journal of Transportation Research.

Lorenzo Mussone held a master degree in electronic engineering in 1982 and a PhD in transportation engineering in 1995. Since 2011, he is an associate professor at Politecnico di Milano. The main scientific activities concern modelling by different techniques: partial derivative macroscopic equations, microscopic simulation, neural networks, swarm intelligence and graph theory, applied to road accident data analysis, vehicular flow control, capacity of complex railway systems, driver behaviour study, roundabouts design, transportation network analysis, and ITS applications. He is in the panel of reviewers of many transportation journals. Since 2005, he is in the editorial board of Accident Analysis & Prevention journal and Transportation Research Interdisciplinary Perspectives.

Conflict of Interest and Authorship Conformation Form

Please check the following as appropriate:

- X All authors have participated in (a) conception and design, or analysis and interpretation of the data; (b) drafting the article or revising it critically for important intellectual content; and (c) approval of the final version.
- X This manuscript has not been submitted to, nor is under review at, another journal or other publishing venue.
- X The authors have no affiliation with any organization with a direct or indirect financial interest in the subject matter discussed in the manuscript
- o The following authors have affiliations with organizations with direct or indirect financial interest in the subject matter discussed in the manuscript:

| Author's name | Affiliation |
|---|---|
| Lorenzo Mussone | Politecnico di Milano, Italy |
| Marco Bassani | Politecnico di Torino, Italy |
| | |
| | |
| | |
| | |
| | |
| | |